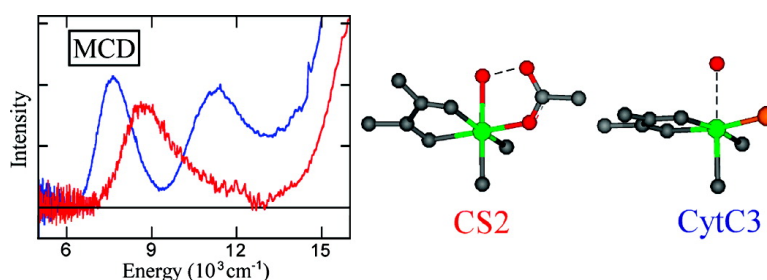


CD and MCD of CytC3 and Taurine Dioxygenase: Role of the Facial Triad in α -KG-Dependent Oxygenases

Michael L. Neidig, Christina D. Brown, Kenneth M. Light, Danica Galoni Fujimori, Elizabeth M. Nolan, John C. Price, Eric W. Barr, J. Martin Bollinger, Carsten Krebs, Christopher T. Walsh, and Edward I. Solomon

J. Am. Chem. Soc., **2007**, 129 (46), 14224-14231 • DOI: 10.1021/ja074557r • Publication Date (Web): 30 October 2007

Downloaded from <http://pubs.acs.org> on February 13, 2009



More About This Article

Additional resources and features associated with this article are available within the HTML version:

- Supporting Information
- Links to the 4 articles that cite this article, as of the time of this article download
- Access to high resolution figures
- Links to articles and content related to this article
- Copyright permission to reproduce figures and/or text from this article

[View the Full Text HTML](#)

CD and MCD of CytC3 and Taurine Dioxygenase: Role of the Facial Triad in α -KG-Dependent Oxygenases

Michael L. Neidig,[†] Christina D. Brown,[†] Kenneth M. Light,[†]
Danica Galonić Fujimori,[‡] Elizabeth M. Nolan,[‡] John C. Price,[§] Eric W. Barr,[§]
J. Martin Bollinger, Jr.,^{§,||} Carsten Krebs,^{§,||} Christopher T. Walsh,[‡] and
Edward I. Solomon^{*,†}

Contribution from the Department of Chemistry, Stanford University, Stanford, California 94305, Department of Biological Chemistry and Molecular Pharmacology, Harvard Medical School, Boston, Massachusetts 02115, and Departments of Biochemistry and Molecular Biology and Chemistry, The Pennsylvania State University, University Park, Pennsylvania 16802

Received June 21, 2007; E-mail: edward.solomon@stanford.edu

Abstract: The α -ketoglutarate (α -KG)-dependent oxygenases are a large and diverse class of mononuclear non-heme iron enzymes that require Fe^{II}, α -KG, and dioxygen for catalysis with the α -KG cosubstrate supplying the additional reducing equivalents for oxygen activation. While these systems exhibit a diverse array of reactivities (i.e., hydroxylation, desaturation, ring closure, etc.), they all share a common structural motif at the Fe^{II} active site, termed the 2-His-1-carboxylate facial triad. Recently, a new subclass of α -KG-dependent oxygenases has been identified that exhibits novel reactivity, the oxidative halogenation of unactivated carbon centers. These enzymes are also structurally unique in that they do not contain the standard facial triad, as a Cl⁻ ligand is coordinated in place of the carboxylate. An Fe^{II} methodology involving CD, MCD, and VTVH MCD spectroscopies was applied to CytC3 to elucidate the active-site structural effects of this perturbation of the coordination sphere. A significant decrease in the affinity of Fe^{II} for apo-CytC3 was observed, supporting the necessity of the facial triad for iron coordination to form the resting site. In addition, interesting differences observed in the Fe^{II}/ α -KG complex relative to the cognate complex in other α -KG-dependent oxygenases indicate the presence of a distorted 6C site with a weak water ligand. Combined with parallel studies of taurine dioxygenase and past studies of clavamate synthase, these results define a role of the carboxylate ligand of the facial triad in stabilizing water coordination via a H-bonding interaction between the noncoordinating oxygen of the carboxylate and the coordinated water. These studies provide initial insight into the active-site features that favor chlorination by CytC3 over the hydroxylation reactions occurring in related enzymes.

Introduction

Oxygen-activating mononuclear non-heme iron enzymes catalyze reactions of medical, pharmaceutical, and environmental significance as diverse as those of heme enzymes.^{1, 2} These systems utilize an Fe^{II} resting site that directly binds O₂ to yield iron–oxygen intermediates that react with substrate to yield product. As the one electron reduction of dioxygen is unfavorable because of its low redox potential and the resulting weak Fe^{III}–O₂⁻ bond that would form,³ these enzymes can be classified on the basis of the source of the extra reducing equivalents required for oxygen activation.⁴ These classes

include the extradiol dioxygenases, pterin-dependent hydroxylase Rieske dioxygenases, and the α -ketoglutarate (α -KG)-dependent oxygenases. Almost all O₂-activating mononuclear non-heme iron enzymes share a common structural motif at the Fe^{II} active site, termed the 2-His-1-carboxylate facial triad, where the ligation sphere of the resting Fe^{II} site consists of two histidines and one carboxylate ligand from the amino acid backbone arranged on one face of an octahedron.^{5–7} The role of this facial triad is to provide three amino acid ligands for iron binding. The three coordination positions not taken up by amino acid ligands (occupied by water) are believed to provide labile sites to bind substrates and cosubstrates (including dioxygen) together for catalysis.

The α -KG-dependent oxygenases require Fe^{II}, α -KG, and dioxygen for catalysis with the α -KG cosubstrate supplying the additional reducing equivalents for oxygen activation.¹ Enzymes in this class catalyze a wide array of chemical transformations,

[†] Stanford University.

[‡] Harvard Medical School.

[§] Department of Biochemistry and Molecular Biology, The Pennsylvania State University.

^{||} Department of Chemistry, The Pennsylvania State University.

(1) Solomon, E. I.; Brunold, T. C.; Davis, M. I.; Kemsley, J. N.; Lee, S.-K.; Lehnert, N.; Neese, F.; Skulan, A. J.; Yang, Y.-S.; Zhou, J. *Chem. Rev.* **2000**, *100*, 235–349.

(2) Que, L.; Ho, R. Y. N. *Chem. Rev.* **1996**, *96*, 2607–2624.

(3) Schenk, G.; Pau, M. Y. M.; Solomon, E. I. *J. Am. Chem. Soc.* **2004**, *126*, 505–515.

(4) Neidig, M. L.; Solomon, E. I. *Chem. Commun.* **2005**, 5843–5863.

(5) Hegg, E. L.; Que, L., Jr. *Eur. J. Biochem.* **1997**, *250*, 625–629.

(6) Que, L. *Nat. Struct. Biol.* **2000**, *7*, 182–184.

(7) Koehntop, K. D.; Emerson, J. P.; Que, L. J. *Biol. Inorg. Chem.* **2005**, *10*, 87–93.

including hydroxylation (prolyl-4-hydroxylase, taurine dioxygenase, TauD), desaturation and oxidative ring closure (clavaminate synthase, CS2), and oxidative ring expansion (deacetoxycephalosporin C synthase).^{1,2} Enzymes in this class are proposed to share a common mechanism involving oxidation of substrate with concomitant two-electron oxidation of α -ketoglutarate to succinate and CO₂, where one atom of O₂ is incorporated into product (or H₂O for ring closure and desaturation reactions) and the other appears in succinate. In these systems, the resting enzyme and complexes with either the substrate or α -KG are all six-coordinate (6C) shown by circular dichroism (CD) and magnetic circular dichroism (MCD) spectroscopy^{8–10} and crystallographic studies.^{11–14} α -KG coordinates directly to the Fe^{II} site in a bidentate fashion. Binding of both α -KG and substrate leads to conversion to a five-coordinate (5C) site, which reacts with O₂ leading to decarboxylation of the α -keto acid to generate CO₂, succinate, and an Fe^{IV}=O intermediate. The latter was trapped and characterized in two α -KG-dependent dioxygenases, TauD¹⁵ and prolyl-4-hydroxylase,¹⁶ and identified as an Fe^{IV}=O species. This intermediate reacts with substrate by H-atom abstraction, as demonstrated by the large deuterium kinetic isotope effects for decay of the intermediates.^{16,17} Formal recombination of a hydroxyl radical equivalent from the Fe^{III}–OH species with the substrate radical yields hydroxylated product. The latter process is known as the oxygen rebound mechanism.¹⁸

Recently, a new subclass of α -KG-dependent oxygenases has been identified whose members exhibit a novel reactivity, the oxidative halogenation of unactivated aliphatic carbon centers in the biosynthesis of several natural products of nonribosomal peptide origin.^{19,20} In these enzymes, the amino acid substrates that are halogenated are first activated by an adenylation domain (A) followed by loading onto the phosphopantetheinyl arm of the thiolation module (T), resulting in an aminoacyl–S–T protein that is the enzyme substrate. Examples include SyrB2, which catalyzes the chlorination of the γ -methyl group of L-threonine tethered to the A–T didomain protein SyrB1,¹⁹ and CytC3, which catalyzes the chlorination of the γ -methyl group of L-2-aminobutyric acid (L-Aba) tethered to the carrier protein CytC2 (i.e., L-Aba-S-CytC2).²⁰ Current structural insight into the active sites of these enzymes derives from crystallographic

studies of SyrB2. From the crystal structure of SyrB2/Fe^{II}/Cl[–]/ α -KG, the Fe^{II} active site is six-coordinate (6C) with a bidentate α -KG ligand, two histidines, a water, and a Cl[–] coordinated to iron.²¹ In this structure, the observed Fe^{II}–Cl bond length of \sim 2.44 Å was suggested to be slightly elongated. Thus, in addition to its novel reactivity, SyrB2 is structurally unique among the oxygen-activating mononuclear non-heme iron enzymes characterized at present, as it does not contain the classic 2-His-L-carboxylate facial triad. Another α -KG-dependent halogenase, CytC3, from *Streptomyces* was studied by a combination of kinetic and spectroscopic methods.²² In contrast to the α -KG-dependent hydroxylases, for which one Fe^{IV}=O species was observed, two high-spin Fe^{IV} species (presumably also Fe^{IV}=O species, although the presence of this group has not yet been demonstrated directly) have been observed in the chlorination reaction catalyzed by CytC3. At least one of these Fe^{IV} complexes cleaves the target C–H bond of the substrate, as evidenced by the large deuterium kinetic isotope effect on decay of the two intermediates.

A methodology developed in our laboratory, employing a combination of near-infrared CD, MCD, and variable-temperature, variable-field (VTVH) MCD spectroscopies, provides a way to directly study $S = 2$ mononuclear non-heme Fe^{II} sites found in these and other enzymes.^{23,24} Previously, this methodology was utilized to gain insight into the active-site structure of the α -KG-dependent oxygenase CS2.^{8–10} In addition, UV/vis MCD provided insight into the metal-to-ligand charge transfer (MLCT) transitions occurring in CS2 in its complex with α -KG. In the present study, this methodology has been utilized to investigate active-site structural effects due to changes in the facial triad. Application to the α -KG-dependent halogenase, CytC3, has revealed interesting active-site differences relative to CS2. Comparison with data from a parallel study of another α -KG-dependent oxygenase, TauD, provides insight into the CytC3 data and suggests an additional role of the facial triad in the O₂ activation mechanism.

Materials and Methods

Overexpression and Purification of Proteins. The adenylation domain protein, CytC1, and the apo form of the thiolation domain protein, CytC2, were purified by a modified version of the described protocol: following elution from the Ni-NTA resin,²⁰ the proteins were loaded onto a gel filtration column (26/60 Superdex 200 for CytC1 and 26/60 Superdex 75 for apoCytC2), eluted in 100 mM Hepes, pH 7.5, concentrated, frozen in liquid nitrogen, and stored at -80 °C. The apo (iron-free) form of the halogenase, CytC3, was overproduced and purified in analogy to the published protocol,²⁰ with the exception that the iron-reconstitution step was omitted. The holo form of CytC2 was prepared via incubation of apo-CytC2 (335 μ M) with MgCl₂ (15 mM), coenzyme A (1.5 mM), and phosphopantetheinyl transferase Sfp (3.7 μ M) in 20 mM Hepes pH 7.5 at 23 °C for 1.5 h. The mixture was subsequently concentrated and then loaded on to a 26/60 Superdex 75 column equilibrated in 20 mM Hepes, pH 7.5. Eluted holo-CytC2 (monomer) was concentrated, frozen in liquid nitrogen, and stored at -80 °C.²⁰

- (8) Pavel, E. G.; Zhou, J.; Busby, R. W.; Gunsior, M.; Townsend, C. A.; Solomon, E. I. *J. Am. Chem. Soc.* **1998**, *120*, 743–753.
- (9) Zhou, J.; Gunsior, M.; Bachmann, B. O.; Townsend, C. A.; Solomon, E. I. *J. Am. Chem. Soc.* **1998**, *120*, 13539–13540.
- (10) Zhou, J.; Kelly, W. L.; Bachman, B. O.; Gunsior, M.; Townsend, C. A.; Solomon, E. I. *J. Am. Chem. Soc.* **2001**, *123*, 7388–7398.
- (11) Valegard, K.; Vanschellinga, A. C. T.; Lloyd, M. D.; Hara, T.; Ramaswamy, S.; Perrakis, A.; Thompson, A.; Lee, H. J.; Baldwin, J. E.; Schofield, C. J.; Hajdu, J.; Andersson, I. *Nature* **1998**, *394*, 805–809.
- (12) Zhang, Z. H.; Ren, J. S.; Stammers, D. K.; Baldwin, J. E.; Harlos, K.; Schofield, C. J. *Nat. Struct. Biol.* **2000**, *7*, 127–133.
- (13) Elkins, J. M.; Ryle, M. J.; Clifton, I. J.; Hotopp, J. C. D.; Lloyd, J. S.; Burzlaff, N. I.; Baldwin, J. E.; Hausinger, R. P.; Roach, P. L. *Biochemistry* **2002**, *41*, 5185–5192.
- (14) Elkins, J. M.; Hewitson, K. S.; McNeill, L. A.; Seibel, J. F.; Schlemminger, I.; Pugh, C. W.; Ratcliffe, P. J.; Schofield, C. J. *J. Biol. Chem.* **2003**, *278*, 1802–1806.
- (15) Price, J. C.; Barr, E. W.; Tirupati, B.; Bollinger, J. M.; Krebs, C. *Biochemistry* **2003**, *42*, 7497–7508.
- (16) Hoffart, L. M.; Barr, E. W.; Guyer, R. B.; Bollinger, J. M., Jr.; Krebs, C. *Proc. Natl. Acad. Sci. U.S.A.* **2006**, *103*, 14738–14743.
- (17) Price, J. C.; Barr, E. W.; Glass, T. E.; Krebs, C.; Bollinger, J. M. *J. Am. Chem. Soc.* **2003**, *125*, 13008–13009.
- (18) Groves, J. T. *J. Chem. Educ.* **1985**, *62*, 928–931.
- (19) Vaillancourt, F. H.; Yin, J.; Walsh, C. T. *Proc. Natl. Acad. Sci. U.S.A.* **2005**, *102*, 10111–10116.
- (20) Ueki, M.; Galonic, D. P.; Vaillancourt, F. H.; Garneau-Tsodikova, S.; Yeh, E.; Vosburg, D. A.; Schroeder, F. C.; Osada, H.; Walsh, C. T. *Chem. Biol.* **2006**, *13*, 1183–1191.

- (21) Blasiak, L. C.; Vaillancourt, F. H.; Walsh, C. T.; Drennan, C. L. *Nature* **2006**, *440*, 368–371.
- (22) Galonic, D. P.; Barr, E. W.; Walsh, C. T.; Bollinger, J. M.; Krebs, C. *Nat. Chem. Biol.* **2007**, *3*, 113–116.
- (23) Solomon, E. I.; Pavel, E. G.; Loeb, K. E.; Campochiaro, C. *Coord. Chem. Rev.* **1995**, *144*, 369–460.
- (24) Pavel, E. G.; Kitajima, N.; Solomon, E. I. *J. Am. Chem. Soc.* **1998**, *120*, 3949–3962.

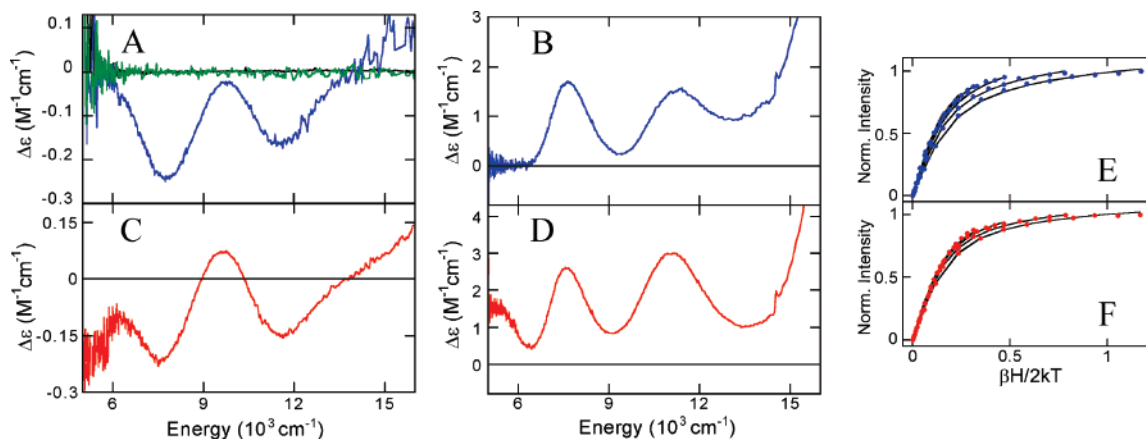


Figure 1. 298 K CD spectra of (A) apoCytC3 (black), apoCytC3/Cl⁻ + 2 equiv of Fe^{II} (green), and CytC3/Fe^{II}/Cl⁻/α-KG (blue) and (C) CytC3/Fe^{II}/Cl⁻/α-KG/L-Aba-S-CytC2. The low-temperature, 7T MCD spectra of (B) CytC3/Fe^{II}/Cl⁻/α-KG and (D) CytC3/Fe^{II}/Cl⁻/α-KG/L-Aba-S-CytC2. VTVH data (symbols) and their best fit (lines) for (E) CytC3/Fe^{II}/Cl⁻/α-KG collected at 7505 cm⁻¹ and (F) CytC3/Fe^{II}/Cl⁻/α-KG/L-Aba-S-CytC2 collected at 7225 cm⁻¹.

TauD was overexpressed and purified as previously described.¹⁵

Preparation of L-Aba-S-CytC2 Substrate. The thiolation domain of CytC2 was post-translationally modified with the phosphopantetheinyl group by incubation with purified Sfp protein and coenzyme A, generating holo-CytC2. Incubation of L-Aba with holo-CytC2 in the presence of CytC1, MgCl₂, and ATP in 100 mM HEPES, pH 7.5, at 23 °C for 1.5 h as previously described generated L-Aba-S-CytC2.²² The amino acid-loaded CytC2 substrate was then concentrated, exchanged into deuterated HEPES buffer (100 mM, pD 7.5), and deoxygenated before addition to CytC3.

CD and MCD Spectroscopy. All samples for spectroscopy were prepared under inert atmosphere inside a N₂-purged “wet box”. Apo-CytC3 was exchanged into deuterated HEPES buffer (100 mM, pD 7.5) and concentrated to 3.0–3.5 mM by using a 4-mL Ultrafree-4 ultrafiltration cell with a 10 kDa cutoff membrane. The enzyme was made anaerobic by purging with argon gas on a Schlenk line at 0 °C for 1 h. NaCl (1 M), ferrous ammonium sulfate (120 mM), α-KG (1 M), and L-Aba-S-CytC2 (3.78 mM) were added in microliter quantities from anaerobic stock solutions in degassed HEPES buffer (100 mM, pD 7.5). For cofactor and substrate binding, microliter additions were made until no further changes in the spectra were observed to ensure saturation. The same procedure was followed for TauD with deuterated TrisHCl buffer (100 mM, pD 7.5) and stock solutions of ferrous ammonium sulfate (120 mM), α-KG (1 M), and taurine (250 mM). Glycerol-*d*₃ was added to 50–60% (v/v) to the enzyme solutions for preparation of MCD samples to give MCD samples of 1.0–1.5 mM concentration. CD spectra were taken without and with glycerol addition to ensure that the Fe^{II} site was unaffected by the glassing agent.

Near-IR (600–2000 nm) CD and MCD data were recorded on a Jasco J-200D spectropolarimeter with a liquid N₂-cooled InSb detector and equipped with an Oxford Instruments SM4000-7 tesla (T) superconducting magnet. UV/vis (300–900 nm) MCD data were recorded on a Jasco J810 spectropolarimeter with an extended S-20 photomultiplier tube and equipped with an Oxford Instruments SM4000-7T superconducting magnet. CD spectra were corrected for buffer and cell baselines by subtraction, and MCD spectra were corrected for the natural CD and zero-field baseline effects by averaging the positive and negative field data at a given temperature. VTVH MCD data were collected using a calibrated Cernox resistor (Lakeshore Cryogenics, calibrated 1.5–300 K) inserted into the sample cell to accurately measure the sample temperature. VTVH MCD data were normalized to the maximum observed intensity over all isotherms for a given wavelength, and the ground-state parameters were extracted by fitting in accordance with published procedures.^{23,24}

Results and Analysis

The energies and splitting pattern of CD/MCD bands provide information about the geometric and electronic structure of the ferrous active sites in CytC3 and TauD. In octahedral symmetry, a 6C ferrous site has a doubly degenerate ⁵E_g ligand field (LF) excited state and a triply degenerate ⁵T_{2g} ligand field ground state split in energy by 10 *Dq* ≈ 10 000 cm⁻¹ for biologically relevant nitrogen and oxygen ligands. In the low symmetry of a protein active site, these states further split (⁵E_g → *d*_{x²-y² and *d*_{z²}) resulting in two ligand field transitions centered at ~10 000 cm⁻¹, split by ~2000 cm⁻¹ for a distorted 6C ferrous site. Five-coordinate (5C) square-pyramidal sites show these transitions at ~10 000 and ~5000 cm⁻¹, and 5C trigonal bipyramidal sites exhibit one transition at <10 000 cm⁻¹ and one at <5000 cm⁻¹. Distorted four-coordinate sites show only low-energy ligand field transitions in the 4000–7000 cm⁻¹ region, due to the much smaller value of 10 *Dq* for tetrahedral complexes (10 *Dq* (T_d) = -4/9 10 *Dq* (O_h)).^{23,24}}

(I) CytC3. The 278 K CD spectrum of apo-CytC3 in the presence of 50 equiv of Cl⁻ is featureless (Figure 1A, black). Addition of up to 2 equiv of Fe^{II} to apo-CytC3/Cl⁻ results in no observable LF features in the CD spectrum (Figure 1A, green), indicating that Fe^{II} does not bind to apo-CytC3/Cl⁻. Further addition of Fe^{II} leads to enzyme precipitation. Considering both the minimal CD signal observable above baseline and the previous Δε values observed for the CD spectra of resting ferrous active sites of mononuclear non-heme iron enzymes, a maximum (association) binding constant for Fe^{II} to apo-CytC3/Cl⁻ can be estimated to be <50 M⁻¹. This binding constant is significantly reduced (by >2 orders of magnitude) from that previously determined by near-infrared CD titration for another α-KG-dependent oxygenase, CS2 (*K*_B > 5000 M⁻¹).⁸

While Fe^{II} does not bind to apo-CytC3/Cl⁻, addition of 25 equiv of α-KG (saturating) to apo-CytC3/Cl⁻ + 0.9 equiv of Fe^{II} results in Fe^{II} binding to the active site, as the CD spectrum now contains negative bands at ~7760 cm⁻¹ and ~11 550 cm⁻¹ (Figure 1A, blue). Thus, α-KG significantly increases the binding affinity of the active site of CytC3 for Fe^{II} (by at least 2 orders of magnitude compared to that for CytC3 in the absence of α-KG). (The binding affinity was estimated considering the maximum MCD intensity for free Fe^{II} in solution that would

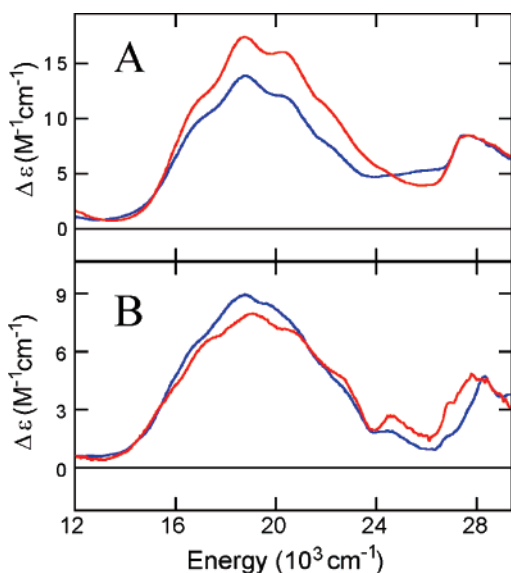


Figure 2. Low-temperature, 7T UV/vis MCD spectra of (A) CytC3/Fe^{II}/Cl⁻/α-KG (blue) and CytC3/Fe^{II}/Cl⁻/α-KG/L-Aba-S-CytC2 (red) and (B) TauD/Fe^{II}/α-KG (blue) and TauD/Fe^{II}/α-KG/taurine (red).

be observable and the CD intensity observed, utilizing typical $\Delta\epsilon$ values for α-KG-bound complexes in other enzymes.) The 5 K, 7T MCD spectrum of CytC3/Fe^{II}/Cl⁻/α-KG (Figure 1B) contains positive LF features at ~ 7640 and $\sim 11\,300$ cm⁻¹. In addition, an Fe^{II} \rightarrow α-KG CT band at $>15\,000$ cm⁻¹ is observed, indicating direct bidentate coordination of α-KG to Fe^{II} (Figure 2). The presence of two LF transitions at these energies is consistent with a distorted 6C Fe^{II} site. The larger splitting of these bands ($\Delta^5E_g \approx 3460$ cm⁻¹) compared to the typical ⁵E_g splitting for distorted 6C sites (~ 2000 cm⁻¹) is consistent with one of the six ligands (likely H₂O) being weakly coordinated.

To evaluate the ligand field effects of replacing the carboxylate ligand of the facial triad with a chloride anion on the d \rightarrow d transition energies, the Companion–Komarynsky method was employed.²⁵ An absorption spectrum of *trans*-Fe(py)₄Cl₂ was used to obtain ligand field parameters for chloride in a charge-neutral complex at a bond distance of 2.4 Å,²⁶ conditions that closely match those found in CytC3. Note that this bond length is also within the range reported for high-spin six-coordinate Fe^{II} complexes with two anionic ligands.^{27–31} Ligand field parameters for histidine, water, and carboxylate were obtained from previous studies as listed in ref 23. These latter parameters, when used to model the resting site of CS2, gave d orbital splittings that were in good agreement with experiment. (The ligand field parameters used were: His: $\alpha_2 = 19\,185$ cm⁻¹, $\alpha_4 = 7010$ cm⁻¹; carboxylate: $\alpha_2 = 17\,000$ cm⁻¹, $\alpha_4 = 5800$ cm⁻¹; water: $\alpha_2 = 18\,000$ cm⁻¹, $\alpha_4 = 5680$ cm⁻¹; chloride:

$\alpha_2 = 17\,730$ cm⁻¹, $\alpha_4 = 4690$ cm⁻¹; α-KG carbonyl: $\alpha_2 = 17\,700$ cm⁻¹, $\alpha_4 = 5300$ cm⁻¹; α-KG carboxylate: $\alpha_2 = 17\,250$ cm⁻¹, $\alpha_4 = 5600$ cm⁻¹. Ligand field calculated vs experimental energies for CS2 ($d_{xz} \equiv 0$ cm⁻¹): Calculated: $d_{yz} = 0$ cm⁻¹, $d_{xy} = 650$ cm⁻¹, $d_z^2 = 9690$ cm⁻¹, $d_{x^2-y^2} = 11\,220$ cm⁻¹. Experimental: $d_{yz} = 190$ cm⁻¹, $d_{xy} = 495$ cm⁻¹, $d_z^2 = 9210$ cm⁻¹, $d_{x^2-y^2} = 10\,900$ cm⁻¹.)

The α-KG-bound form of CS2 was approximated by replacing the waters of the previous model with the parameters of a strengthened amide carbonyl and a weakened carboxylate. Again the orbital splittings matched well with those from experiment. Replacement of the ligand field parameters of the facial triad carboxylate with those of chloride led to a decrease, not increase, in the ⁵E_g excited-state splitting of 150 cm⁻¹ (from 1620 cm⁻¹ for the facial triad to 1470 cm⁻¹). Therefore, this substitution of chloride for carboxylate cannot be the source of the large excited-state splitting in CytC3, which is instead attributed to a weak water ligand.

The saturation magnetization MCD behavior for CytC3/Fe^{II}/Cl⁻/α-KG collected at 7505 cm⁻¹ (Figure 1E) is well described by a negative zero-field splitting (ZFS) non-Kramers doublet model with ground-state spin-Hamiltonian parameters of $\delta = 2.8 \pm 0.2$ cm⁻¹ and $g_{||} = 8.9 \pm 0.3$ cm⁻¹ (δ is the ZFS of the $S = 2$, $M_s = \pm 2$ doublet, and $g_{||}$ defines its Zeeman splitting). These values of δ and $g_{||}$ give $\Delta = -900 \pm 150$ cm⁻¹ and $|V/2\Delta| = 0.28$, which reflect the axial ($E_{xz,yz} - E_{xy} = \Delta$) and rhombic ($E_{xz} - E_{yz} = V$) splitting of the t_{2g} set of d π orbitals on the Fe^{II}. The large observed splitting of the ⁵T_{2g} ground state is consistent with backbonding between Fe^{II} and the bound α-KG, as previously observed for CS2/Fe^{II}/α-KG.⁸

The 5 K, 7T UV/vis MCD spectrum of CytC3/Fe^{II}/Cl⁻/α-KG (Figure 2A, blue) is nearly identical to that previously reported for other α-KG-dependent oxygenases (e.g., CS2¹³) with MLCT and n \rightarrow π^* transitions at $\sim 19\,100$ and $\sim 28\,000$ cm⁻¹, respectively. Previous studies have shown that these transitions arise from bidentate coordination of α-KG to Fe^{II}.⁸ Thus, CD and MCD spectroscopic studies indicate that CytC3/Fe^{II}/Cl⁻/α-KG is a distorted 6C Fe^{II} site with a weak ligand (likely water) and a bidentately coordinated α-KG cofactor.

Addition of 2.5 equiv of L-Aba-S-CytC2 substrate (saturating) to CytC3/Fe^{II}/Cl⁻/α-KG results in a different CD spectrum with a low-energy negative feature at <5000 cm⁻¹, two additional negative features at ~ 7560 and ~ 11650 cm⁻¹, and a positive band at ~ 9660 cm⁻¹ (Figure 1C). The 5 K, 7T MCD spectrum of substrate-bound CytC3/Fe^{II}/Cl⁻/α-KG/L-Aba-S-CytC2 (Figure 1D) contains a positive LF feature at <5000 cm⁻¹ and additional positive LF features at ~ 7600 and $\sim 11\,070$ cm⁻¹. In addition, an Fe^{II} \rightarrow α-KG CT band at $>15\,000$ cm⁻¹ is observed, indicating that α-KG remains directly coordinated to Fe^{II} upon substrate binding (Figure 2). The observation of at least three features in the MCD spectrum of CytC3/Fe^{II}/Cl⁻/α-KG/L-Aba-S-CytC2 indicates the presence of two distinct ferrous species, since LF theory and experiment dictate that a single Fe^{II} site can have no more than two d \rightarrow d transitions in this region. Because of its energy position, the ~ 7600 band corresponds to a 6C component, whereas the low energy of the LF transition at <5000 cm⁻¹ indicates that it is associated with a 5C component. VTVH MCD data (vide infra) indicate that the positive bands at $\sim 11\,070$ and ~ 7600 cm⁻¹ arise from different ferrous species, likely reflecting contributions of two

(25) Companion, A.; Komarynsky, C. *J. Chem. Educ.* **1964**, *41*, 257–262.

(26) Little, B.; Long, G. *Inorg. Chem.* **1978**, *17*, 3401–3413.

(27) Batten, M. P.; Cauty, A. J.; Cavell, K. J.; Ruther, T.; Skelton, B. W.; White, A. H. *Acta Crystallogr.* **2004**, *C60*, m316–m319.

(28) Hubin, T. J.; McCormick, J. M.; Collinson, S. R.; Buchalova, M.; Perkins, C. M.; Alcock, N. W.; Kahol, P. K.; Raghunathan, A.; Busch, D. H. *J. Am. Chem. Soc.* **2000**, *122*, 2512–2522.

(29) Hardman, N. J.; Fang, X.; Scott, B. L.; Wright, R. J.; Martin, R. L.; Kubas, G. J. *Inorg. Chem.* **2005**, *44*, 8306–8316.

(30) Halfen, J. A.; Moore, H. L.; Fox, B. G. *Inorg. Chem.* **2002**, *41*, 3935–3943.

(31) Nunes, G. G.; Bottini, R. C. R.; Reis, D. M.; Camargo, P. H. C.; Evans, D. J.; Hitchcock, P. B.; Leigh, G. J.; Sa, E. L.; Soares, J. F. *Inorg. Chim. Acta* **2004**, *357*, 1219–1228.

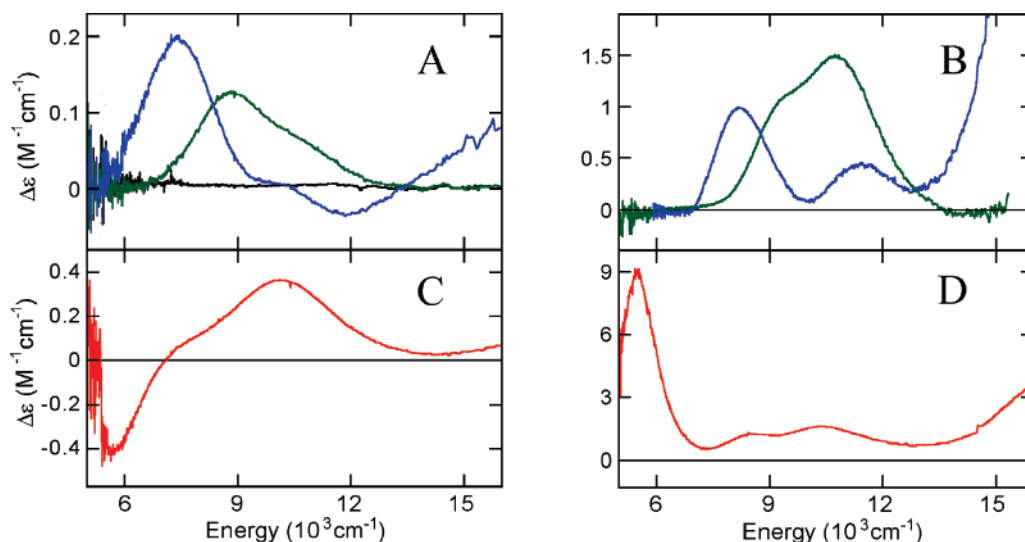


Figure 3. 298 K CD spectra of (A) apoTauD (black), TauD/Fe^{II} (green), and TauD/Fe^{II}/α-KG (blue) and (C) TauD/Fe^{II}/α-KG/taurine. The low-temperature, 7T MCD spectra of (B) TauD/Fe^{II} (green) and TauD/Fe^{II}/α-KG (blue) and (D) TauD/Fe^{II}/α-KG/taurine.

overlapping bands at this energy (i.e., the higher energy $d \rightarrow d$ bands for both the 5C and 6C components).

The saturation magnetization behavior for CytC3/Fe^{II}/Cl⁻/α-KG/L-Aba-S-CytC2 collected at 7225 cm⁻¹ (the 6C component, Figure 1F) is well described as a negative ZFS non-Kramers doublet with ground-state spin Hamiltonian parameters of $\delta = 2.1 \pm 0.2$ cm⁻¹ and $g_{||} = 8.8 \pm 0.3$ cm⁻¹, corresponding to $\Delta = -1200 \pm 150$ cm⁻¹ and $|V/2\Delta| = 0.28$. The large observed splitting of the ⁵T_{2g} ground state is consistent with analogous backbonding between Fe^{II} and the bound α-KG as observed for CytC3/Fe^{II}/Cl⁻/α-KG. The decreased nesting observed for this band in the substrate-bound complex compared to that for the analogous band in the α-KG complex indicates that the 6C species is perturbed upon substrate binding. The saturation magnetization behavior at 11 085 cm⁻¹ is significantly more nested (Supporting Information, Figure S1) and cannot be fit to any single set of spin-Hamiltonian parameters, consistent with the presence of overlapping bands at this energy. Therefore, the positive bands at ~7600 and ~11 070 cm⁻¹ in Figure 1D are associated with different α-KG and substrate-bound ferrous active sites indicating the presence of a mixture of 5C and 6C species in the enzyme–substrate (ES) complex.

The 5 K, 7T UV/vis MCD spectrum of CytC3/Fe^{II}/Cl⁻/α-KG/L-Aba-S-CytC2 (Figure 2A, red) is nearly identical to that observed for CytC3/Fe^{II}/Cl⁻/α-KG with MLCT and $n \rightarrow \pi^*$ transitions at ~19 100 and ~28 000 cm⁻¹, respectively, indicating that substrate binding does not affect the α-KG coordination to Fe^{II}. Thus, a combination of CD, MCD, and VTVH MCD studies shows that the ES complex of CytC3 is a mixture of distinct 5C and 6C species where α-KG is bound to Fe^{II} in a bidentate fashion, indicating that a 6C \rightarrow 5C conversion occurs upon substrate binding analogous to that previously observed for CS2.

(2) TauD. As emphasized earlier, MCD studies of the Fe^{II}/α-KG complex of CytC3 indicate the presence of a 6C ferrous site with a weakly coordinated water ligand. This is in contrast to our previous results for the α-KG complex of CS2, in which the water ligand binds tightly to Fe^{II}. It has been proposed that water coordination to CS2/Fe^{II}/α-KG is stabilized through a hydrogen-bonding interaction between the water ligand and the

noncoordinating oxygen of the carboxylate of the facial triad.¹⁰ This orientation has been observed in the crystal structures of α-KG enzymes in both the presence and absence of substrate.^{12,14,32–35} However, the crystal structure of TauD/Fe^{II}/α-KG with taurine bound is different.^{18,36} In this enzyme structure, the noncoordinating oxygen of the carboxylate ligand is flipped down and away from the open (i.e., water) coordination site. Therefore, the ferrous active site of TauD was investigated to determine if this structural change affected water coordination to the iron.

The 278 K CD spectrum of apoTauD is featureless (Figure 3A, black), whereas addition of 0.9 equiv of Fe^{II} results in a spectrum with two positive LF bands at ~8850 and ~10 600 cm⁻¹ (Figure 3A, green). The 1.8 K, 7T MCD spectrum of TauD/Fe^{II} (Figure 3B, green) also shows two positive ligand field features at ~8900 and ~10 700 cm⁻¹. The observed CD and MCD excited-state splittings and energies of the two transitions of TauD/Fe^{II} are consistent with a distorted 6C resting ferrous site.

Addition of 25 equiv of α-KG (saturating) to resting TauD/Fe^{II} results in a significant change in the CD spectrum, with a positive band at ~7400 cm⁻¹ and a negative band at ~11 150 cm⁻¹ (Figure 3A, blue). The 1.8 K, 7T MCD spectrum of TauD/Fe^{II}/α-KG (Figure 3B, blue) contains positive LF features at ~8190 and ~11 450 cm⁻¹. The presence of two LF transitions at these energies is consistent with a distorted 6C Fe^{II} site. The larger splitting of these bands ($\Delta^5E_g \approx 3260$ cm⁻¹) compared to the typical ⁵E_g splitting for distorted 6C sites (~2000 cm⁻¹) is consistent with one of the six ligands (likely H₂O) being weakly coordinated.

The 1.8 K, 7T UV/vis MCD spectrum of TauD/Fe^{II}/α-KG (Figure 2B, blue) is nearly identical to that previously reported for other α-KG-dependent oxygenases (e.g., CS2⁸) with MLCT

- (32) McDonough, M. A.; Kavanagh, K. L.; Butler, D.; Searles, T.; Oppermann, U.; Schofield, C. J. *J. Biol. Chem.* **2005**, *280*, 41101–41110.
 (33) Valegard, K.; van Scheltinga, A. C.; Lloyd, M. D.; Hara, T.; Ramaswamy, S.; Perrakis, A.; Thompson, A.; Lee, H. J.; Baldwin, J. E.; Schofield, C. J.; Hajdu, J.; Andersson, I. *Nature* **1998**, *394*, 805–809.
 (34) Clifton, I. J.; Doan, L. X.; Sleeman, M. C.; Topf, M.; Suzuki, H.; Wilmouth, R. C.; Schofield, C. J. *J. Biol. Chem.* **2003**, *278*, 20843–20850.
 (35) Wilmouth, R. C.; Turnbull, J. J.; Welford, R. W. D.; Clifton, I. J.; Prescott, A. G.; Schofield, C. J. *Structure* **2002**, *10*, 93–103.
 (36) O'Brien, J.; Schuller, D.; Yang, V.; Dillard, B.; Lanzilotta, W. *Biochemistry* **2003**, *42*, 5547–5554.

and $n \rightarrow \pi^*$ transitions at $\sim 19\,100$ and $\sim 28\,000$ cm^{-1} , respectively, indicating bidentate coordination of α -KG to Fe^{II} . Thus, CD and MCD spectroscopic data indicate that TauD/ Fe^{II} / α -KG is a distorted 6C Fe^{II} site with a weak ligand (likely water) and α -KG cofactor bound in a bidentate fashion.

Addition of 10 equiv of taurine (saturating) to TauD/ Fe^{II} / α -KG results in a different CD spectrum with a negative band at ~ 5000 cm^{-1} and a positive band at $\sim 10\,150$ cm^{-1} (Figure 3C). The 1.8 K, 7T MCD spectrum of TauD/ Fe^{II} / α -KG/taurine (Figure 3D) contains an intense positive LF feature at ~ 5500 cm^{-1} and additional positive bands at ~ 8550 and $\sim 10\,400$ cm^{-1} . The observation of at least three features in the MCD spectrum of TauD/ Fe^{II} / α -KG/taurine indicates the presence of two distinct ferrous species. The low-energy feature at ~ 5500 cm^{-1} indicates that a square-pyramidal 5C Fe^{II} site is one component of the mixture. On the basis of the energy positions of the additional positive bands at 8550 – $10\,400$ cm^{-1} , the other component is a distorted 6C site. The 1.8 K, 7T UV/vis MCD spectrum of TauD/ Fe^{II} / α -KG/taurine (Figure 2B, red) is nearly identical to that for TauD/ Fe^{II} / α -KG with MLCT and $n \rightarrow \pi^*$ transitions at $\sim 19\,300$ and $\sim 28\,000$ cm^{-1} , respectively. Therefore, CD and MCD studies of TauD/ Fe^{II} / α -KG/taurine indicate this species to be a mixture of distinct 5C and 6C ferrous sites with bidentate coordination of α -KG, indicating a $6\text{C} \rightarrow 5\text{C}$ conversion upon substrate binding analogous to that observed for CytC3 and CS2.

Discussion

The 2-His-1-carboxylate facial triad is a ubiquitous active-site structural motif in oxygen-activating mononuclear non-heme iron enzymes. The α -KG-dependent halogenases are structurally different, however, having a Cl^- ligand instead of the facial triad carboxylate. In the present study, CD, MCD, and VTVH MCD spectroscopies have provided insight into the active-site geometric and electronic structures of the α -KG-dependent halogenase CytC3. From a comparison to data on CS2 and parallel studies of TauD, these results provide insight into the role of the facial triad in the α -KG-dependent oxygenases.

A commonly considered role of the facial triad in oxygen-activating mononuclear non-heme iron enzymes is to provide three amino acid ligands at the enzyme active site to tightly bind Fe^{II} . By near-infrared CD, the effect of loss of the carboxylate of the facial triad on Fe^{II} binding to the active site of CytC3 was evaluated. No CD signal due to Fe^{II} binding was observed, giving an estimate for the upper limit for the binding constant of Fe^{II} to apo-CytC3 in the presence of Cl^- that is at least 2 orders of magnitude lower than that for CS2. These results demonstrate the requirement of the facial triad for providing a site for high-affinity Fe^{II} binding. In CytC3, the lack of Fe^{II} binding with only two amino acid ligands is overcome by the addition of the α -KG cosubstrate. Crystallography shows that the α -KG cofactor binds to the active site even in the absence of Fe^{II} and supplies two additional ligands to create a high-affinity iron-binding site.²¹

Importantly, MCD studies of CytC3/ Fe^{II} / Cl^- / α -KG show the presence of a 6C ferrous site with a large $^5\text{E}_g$ splitting ($\Delta^5\text{E}_g \approx 3460$ cm^{-1}), indicating the presence of a weakly coordinated water ligand (Figure 4, blue). This assignment is based upon LF calculations that indicate that the Cl^- ligand (at ~ 2.44 Å from crystallography on the related enzyme SyrB2) would not lead to the large $^5\text{E}_g$ splitting observed. An analogously large

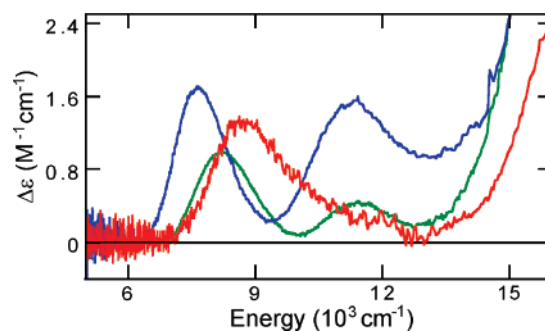


Figure 4. Low-temperature, 7T MCD spectra of CS2/ Fe^{II} / α -KG (red), TauD/ Fe^{II} / α -KG (green) and CytC3/ Fe^{II} / Cl^- / α -KG.

$^5\text{E}_g$ splitting ($\Delta^5\text{E}_g \approx 3260$ cm^{-1}) is also observed in TauD/ Fe^{II} / α -KG and must be due to the presence of a weak water ligand. These results contrast with our previous MCD data for CS2/ Fe^{II} / α -KG, in which the $^5\text{E}_g$ splitting ($\Delta^5\text{E}_g \approx 1630$ cm^{-1}) was consistent with a strong water ligand at the sixth coordination position (Figure 4, red). Given that the resting site of TauD is 6C with water tightly bound to Fe^{II} from MCD, we conclude that it is the bidentate coordination of α -KG cofactor, a good donor (which replaces two water ligands in the resting site), that leads to the weakening of the remaining water ligand in the α -KG complexes.

Although α -KG binding in CS2 could also lead to the weakening of the water ligand, this weakening is not observed, as MCD data show that the water is bound tightly to Fe^{II} even in the presence of α -KG. An active-site feature that can stabilize water binding in CS2 is a H-bonding interaction between the coordinated water and the noncoordinating oxygen of the monodentate carboxylate of the facial triad (observed in the crystal structure of CS2/ Fe^{II} / α -KG¹²). Replacement of this carboxylate ligand in CytC3 by Cl^- eliminates this H-bonding interaction, which could lead to weakening of the water ligand upon α -KG binding. While TauD contains this carboxylate ligand, it appears to be in an orientation (i.e., potentially flipped down as observed in TauD crystallography) that would preclude a stabilizing H-bond with the coordinated water, leading to its weakened ligation. Thus, a role of the facial triad in oxygen-activating mononuclear non-heme iron enzymes appears to be the regulation of water affinity to the site upon α -KG binding through H-bonding to the noncoordinating oxygen of the carboxylate ligand.

Density functional theory calculations were utilized to gain further insight into the contribution of this H-bonding interaction to the water binding to the ferrous site (Figure 5). All complexes were geometry-optimized using the Gaussian 03 software package,³⁷ with the spin-unrestricted BP86 functional^{38,39} with 10% Hartree–Fock exchange under tight convergence criteria. The starting geometry was taken from the crystal structure of TauD/ Fe^{II} / α -KG,¹³ with α -KG truncated to remove the terminal carboxylate. Protein-derived ligands (His-99, His-255, and Asp-101) were truncated with Me-imidazoles modeling histidines and propionate modeling aspartate, and the α -carbons of the protein ligands were frozen relative to each other to mimic the constraints of the protein backbone. Geometry optimizations were carried out using a split basis set of triple- ζ 6-311G* for

(37) Frisch, M. J.; et al. *Gaussian 03*; Gaussian, Inc.: Wallingford, CT, 2004.

(38) Perdew, J. P. *Phys. Rev. B* **1986**, *33*, 8822–8824.

(39) Becke, A. D. *Phys. Rev. A* **1988**, *38*, 3098–3100.

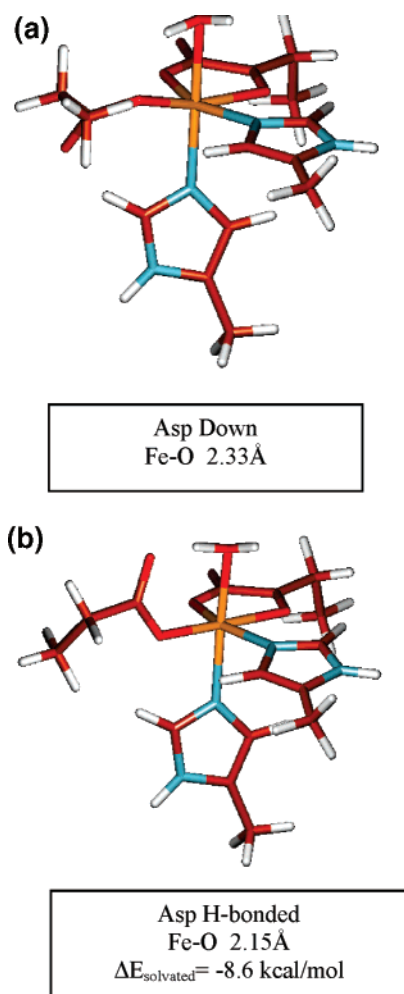


Figure 5. Geometry-optimized structures of TauD/Fe^{II}/α-KG without and with H-bonding to carboxylate.

the iron and the two carbon and three oxygen atoms of the α-keto acid moiety and double- ζ 6-31G* for the remaining atoms. Optimized structures and molecular orbitals were visualized using Molden version 4.1.⁴⁰ Frequencies and thermodynamic parameters were calculated using the split 6-311G*/6-31G* basis set. Energies were determined using single-point calculations with the above functional and split basis set, and solvation effects were considered using the polarized continuum model⁴¹ with a dielectric constant $\epsilon = 4.0$ to model the protein environment.

To estimate the strength of the H-bond, two structures were optimized: one with the carboxylate O in the plane of the α-KG cofactor and the other with the carboxylate rotated to allow for H-bonding to the water ligand. The difference in energy of the two structures was found to be ~ 8.6 kcal/mol, giving an upper estimate of the strength of the H-bond. This strong H-bond is due to the anionic nature of the carboxylate, which also polarizes the O–H bond of the water ligand, leading to more OH[−] character and a shorter Fe–O bond. This H-bonding to the water decreases its binding energy to the 5C Fe^{II} site from $\Delta G = +8.0$ kcal/mol (calculated without the H-bond, Figure 5, left) to $\Delta G = -1.0$ kcal/mol with the H-bond (Figure 5, right). Thus,

the presence of the H-bond to the terminal oxygen of the carboxylate of the facial triad significantly increases the water affinity of the Fe^{II} site.

In α-KG-dependent oxygenases, the presence of a 6C α-KG bound complex is important in preventing an uncoupled reaction in the absence of substrate. From the above results, these enzymes generally maintain the 6C site through H-bonding between the carboxylate ligand and the coordinated water (as for CS2). TauD and CytC3 do not, instead maintaining a weak water ligand in their α-KG complexes that appears to be sufficient to prevent the uncoupled reaction with oxygen. (The weakened water ligand in TauD is sufficient to limit the O₂ reaction as the rate is ~ 1000 -fold faster for TauD/Fe^{II}/α-KG/taurine than for the substrate-free TauD/Fe^{II}/α-KG complex.^{42,43} However, the weakened water ligand is not as effective as a strong water ligand in preventing the uncoupled reaction, as evidenced by the 5-fold increase in rate of the uncoupled reaction for TauD over CS2.^{43,44}) TauD and CytC3 appear to employ additional second sphere interactions to prevent complete loss of water ligation upon α-KG binding, which would generate a 5C site highly susceptible to uncoupled O₂ activation. From crystallography, an Asn residue is present in TauD near the water coordination position that could potentially H-bond to the water to stabilize weak ligation. This residue is absent in the available crystal structures of other α-KG-dependent enzymes. In CytC3, a second sphere H-bonding interaction involving the coordinated Cl[−] and the water ligand via a noncoordinated water could serve the same stabilizing function (according to the structure of the homologous SyrB2).²¹

In addition to defining a role of the carboxylate of the facial triad, CD and MCD studies of substrate binding in CytC3 and TauD provide insight into O₂ activation and the reaction pathways of these enzymes. In both systems, substrate binding leads to similar ES complexes with α-KG bound in a bidentate fashion. The presence of the Cl[−] ligand in the first coordination sphere of CytC3 has little direct effect on the electronic structure of the substrate-bound complex. The observed 6C → 5C conversion of the Fe^{II} sites upon substrate binding to the α-KG complexes provides an open site for O₂ to bind and react, following a common mechanism for O₂-activating mononuclear non-heme iron enzymes that utilize redox active cofactors. Upon O₂ binding to the coordinatively unsaturated Fe^{II} site in the presence of both cosubstrates, these enzymes would proceed along similar reaction coordinates with decarboxylation of the coordinated α-KG leading to a similar iron–oxygen intermediate as has been demonstrated.^{15,22}

It is interesting to consider the possible mechanistic role of the weakened water ligands in CytC3 and TauD compared to CS2 in the 6C → 5C conversion of the Fe^{II} site upon substrate binding required for O₂ activation. From crystallography, the substrate in CS2 binds directly above the water coordination position, leading to the loss of the water ligand to generate the 5C site.¹² In contrast, from crystallography of TauD, substrate (taurine) does not bind directly above the water coordination site but is more off-center.^{13,36} Thus, the bound taurine would

(40) Schaftenaar, G.; Noordik, J. H. *J. Comput.-Aided Mol. Des.* **2000**, *14*, 123–134.

(41) Cramer, C. J.; Truhlar, D. G. *Chem. Rev.* **1999**, *99*, 2161–2200.

(42) Price, J. C. Ph.D. Thesis, The Pennsylvania State University, University Park, PA, 2005.

(43) Ryle, M. J.; Liu, A.; Muthukumaran, R. B.; Ho, R. Y. N.; Koehntop, K. D.; McCracken, J.; Que, L.; Hausinger, R. P. *Biochemistry* **2003**, *42*, 1854–1862.

(44) Salowe, S. P.; Marsh, E. N.; Townsend, C. A. *Biochemistry* **1990**, *29*, 6499–6508.

likely interact more weakly with the coordinated water ligand, and hence, the weakened water ligand in TauD/Fe^{II}/α-KG would facilitate its loss of water upon taurine binding. The presence of a weak water ligand in CytC3 may also be required for the 6C → 5C conversion. The decreased fraction of 5C complex generated in CytC3 upon substrate binding (compared to TauD) indicates that, even with a weak water ligand, L-Aba-S-CytC2 substrate binding is not as efficient in destabilizing the water ligand. One possible explanation is that the CytC3 substrate does not approach as close to the Fe^{II} site as observed in other α-KG-dependent oxygenases, possibly a consequence of its attachment to a carrier protein.

Finally, it is interesting to consider the active-site features that could contribute to the observed chlorination rather than hydroxylation reactivity of CytC3. After H-atom abstraction by the Fe^{IV}=O intermediate generated in the O₂ reaction, the presence of the Cl⁻ ligand in the first coordination sphere of the resulting Fe^{III}-OH⁻ species in CytC3 might allow the site to transfer either a hydroxyl radical (as in TauD) or a chlorine atom to the substrate radical. From our MCD studies, the substrate in CytC3 is likely fairly distant from the iron site, consistent with the reduced rate of C-H bond cleavage for this enzyme.²² In this case, during the rebound reaction the Fe^{III}-L (L = OH⁻ or Cl⁻) bond would largely be broken before formation of the C_{sub}-L bond. Therefore, the relative reaction barriers for rebound hydroxylation versus chlorine atom transfer would depend upon the energetic differences between the homolytic cleavage of an Fe^{III}-OH⁻ bond or an Fe^{III}-Cl⁻ bond. As raised in ref 45, there is a difference in potential and, in addition, a difference in bond dissociation energy (C-Cl < C-OH by ~8–11 kcal/mol in aliphatic and aromatic compounds⁴⁶), both of which will favor chlorination. It is also noteworthy that because the chlorine atom transfer would result

in reduction of the Fe^{III}-OH⁻ species, protonation of the hydroxide ligand to generate an Fe^{II}-OH₂ site would be strongly coupled to and potentially help promote the chlorine transfer.

In summary, CD and MCD spectroscopies have been utilized to elucidate the geometric and electronic structure of the α-KG-dependent halogenase CytC3, which has an unusual Fe^{II} coordination site in which Cl⁻ replaces the carboxylate of the 2-His-1-carboxylate facial triad. This perturbation eliminates Fe^{II} binding to apo-CytC3, supporting the necessity of the facial triad for iron coordination to form the resting site and the role of the α-KG in the chlorinase in forming the catalytic site. Interesting differences in the α-KG complex indicate the presence of a weak water ligand. Combined with parallel studies of TauD and past studies of CS₂, these results define a role of the carboxylate ligand of the facial triad in stabilizing water coordination via a H-bonding interaction between the noncoordinating oxygen of the carboxylate and the coordinated water. Finally, these studies provide initial insight into the active-site features that favor chlorination versus hydroxylation in CytC3.

Acknowledgment. This research was supported by NIH Grants GM40392 (E.I.S.), GM69657 (J.M.B. and C.K.), and GM20011 and GM49338 (C.T.W.), an NIH Postdoctoral Fellowship (E.M.N.), the Damon Runyon Cancer Research Foundation (Postdoctoral Scholarship DRG-1893-05 to D.G.F.), the Arnold and Mabel Beckman Foundation (Young Investigator Award to C.K.), and the Dreyfus Foundation (Camille Dreyfus Teacher Scholar Award to C.K.).

Supporting Information Available: Details of the Companion-Komarynsky calculations, VTVH MCD data for CytC3/Fe^{II}/Cl⁻/α-KG/L-Aba-S-CytC2 collected at 11085 cm⁻¹, and complete ref 37. This material is available free of charge via the Internet at <http://pubs.acs.org>.

JA074557R

(45) Kojima, T.; Leising, R. A.; Yan, S.; Que, L. *J. Am. Chem. Soc.* **1993**, *115*, 11328–11335.

(46) DiLabio, G. A.; Pratt, D. A. *J. Phys. Chem. A* **2000**, *104*, 1938–1943.